Imaging Artifacts

7

Pedro Filipe Ferreira, Peter D. Gatehouse,
Raad H. Mohiaddin, and David N. Firmin

Abstract

Cardiovascular MR offers a large range of applications. Many of these are still currently under active development by the research community, for improved accuracy and reliability.

The complex nature of the cardiovascular system offers many challenges to clinicians. Its unique mixture of respiratory and cardiac motion; fast flowing blood; and the tissue-air interface between the heart and the lungs, are just some of the difficulties faced. Many of these challenges can result in imaging artifacts and measurement errors, which may limit the diagnostic potential of the scan or even contribute to misinterpretation. A good understanding of the physical principles behind the formation of such artifacts is imperative to identifying and minimising them.

This chapter summarises, in a language accessible for a clinical readership, the most problematic artifacts specific to cardiovascular MR, with particular regard to their physical basis, and implications for the different sequences and applications. It includes motion (respiratory, cardiac and blood flow); Gibbs ringing; aliasing; chemical-shift; and B_0-inhomogeneities.

Keywords

Artifacts • Respiratory motion • Cardiac motion • Blood flow • Gibbs • Aliasing • Chemical-shift • Field distortion • Ghosting

Introduction

The anatomical complexity of the chest in addition to the unique cardiac and respiratory motion and fast flowing blood, can lead to *artifacts* which can obscure or easily be misinterpreted as pathology. In this chapter we attempt to summarise some of the most common artifacts found in the wide range of different Cardiovascular Magnetic Resonance (CMR) applications along with possible solutions.

Electronic supplementary material The online version of this chapter (doi:10.1007/978-3-319-22141-0_7) contains supplementary material, which is available to authorized users.

P.F. Ferreira, PhD (✉)
NIHR Cardiovascular Biomedical Research Unit, Royal Brompton Hospital, Sydney Wing, Sydney Street, London SW3 6NP, UK

National Heart and Lung Institute, Imperial College London, London, UK
e-mail: p.ferreira@rbht.nhs.uk

P.D. Gatehouse, PhD • D.N. Firmin
NIHR Cardiovascular Biomedical Research Unit, Royal Brompton Hospital, Sydney Wing, Sydney Street, London SW3 6NP, UK

Department of Cardiac MRI, Royal Brompton Hospital, London, UK

National Heart and Lung Institute, Imperial College London, London, UK
e-mail: p.gatehouse@rbht.nhs.uk; d.firmin@rbht.nhs.uk

R.H. Mohiaddin, MD, FRCR, FRCP, FESC, PhD
NIHR Cardiovascular Biomedical Research Unit, Royal Brompton Hospital, Sydney Wing, Sydney Street, London SW3 6NP, UK

Department of Cardiology and Imaging, National Heart and Lung Institute, Imperial College, London, UK
e-mail: r.mohiaddin@imperial.ac.uk

© Springer International Publishing Switzerland 2015

M.A. Syed et al. (eds.), *Basic Principles of Cardiovascular MRI: Physics and Imaging Technique*,
DOI 10.1007/978-3-319-22141-0_7

An artifact can be defined as something that is visible in an image but it is artificial, and is often detrimental to diagnosis. For this reason it is important to have an understanding of the physical principles behind the formation of such artifacts so that they can be identified and possibly avoided. This chapter focuses on the most problematic artifacts specific to cardiovascular imaging. The causes of these include motion (respiratory, cardiac, and blood flow); Gibbs ringing; aliasing; chemical-shift; and B_0-inhomogeneities. Different artifact sources will be discussed with particular regard to their physical basis and implications for the different sequences and applications.

Motion

The overall motion of the heart is a complex mixture of *cardiac motion* associated with its cyclic pumping and *respiratory motion* that results in an additional twisting and volumetric distortion.

Cardiac motion has been reasonably well controlled over the years by detecting the QRS complex of the ECG and *triggering* the acquisition at a certain delay following this. Evidently ECG triggering works best when there is low variation between beats; arrhythmias and ectopic heart-beats will therefore potentially cause artifacts.

Respiratory motion is relatively unpredictable and can vary considerably from person to person and from time to time. Acquiring the data over the period of a *breath-hold* has in recent years largely controlled it, although this can translate into a long acquisition window within the cardiac cycle, thus potentially including periods of more rapid cardiac motion. Restricting the acquisition to a period of mid diastole where the heart is reasonably still is sometimes not feasible during a breath-hold, especially for patients that have considerable problems in holding their breath longer than a few seconds. For patients with very rapid heart-rates it can also be difficult to find a "motion free" acquisition window. End-expiratory breath-holding is more reproducible but more difficult than end-inspiratory.

Respiratory gating is another technique that allows the removal of gross respiratory motion artifacts by restricting data acquisition to the expiratory pause, thus enabling longer scans with shorter acquisition windows within the cardiac cycle, which in turn reduces cardiac motion problems. Respiratory gating is most commonly used in 3D imaging, in particular in imaging of the coronary arteries due to the high spatial-resolution and coverage required, where breath-hold imaging is impracticable.

A moving object will change both the phase and magnitude of its k-space. Motion during image acquisition will therefore introduce artifacts, and these can be divided into two categories: *intra-view* motion during the acquisition of one phase-encode line, and *inter-view* motion between different phase-encode lines. For most sequences intra-view motion at typical myocardial and respiratory speeds can be ignored, although rapid blood flow in major vessels can be an issue. Inter-view motion artifacts can be caused by cardiac motion and/or breathing motion and are very dependent on the nature of the motion in relation to the k-space coverage.

Motion artifacts can also be created by movement between different components of the sequence, for example between the timing of preparation pulses and image acquisition for a black-blood sequence. The next subsections describe the basics of motion artifacts introduced in cardiac studies and are divided by breathing motion, cardiac motion, and blood flow.

Breathing Motion

Most cardiac sequences are *segmented*, i.e. the acquisition of one image is divided into multiple heartbeats and the acquisition window in each heartbeat is restricted, in order to reduce cardiac motion artifacts and *blurring*. On the other hand, if breath-holding is deficient, respiratory motion will introduce k-space inconsistencies between different segments.

Breathing artifacts will depend on the phase-encoding order used, and the timing of the motion. If, for example, motion only occurred when sampling the edges of k-space, then motion artifacts would result in blurring of the edges of the moving object in the phase encoding direction. If, on the other hand, the central regions of k-space were affected then this would result in a more significant *ghosting* and image degradation (Fig. 7.1). If breathing motion is periodic along the phase-encode direction of k-space, it results in a number of defined "ghost" artifacts distributed in that direction on the image. As can be seen from Fig. 7.1, for acquisition sequences that employ an interleaved segmented coverage of k-space then a single movement or drift in the respiratory position will result in ghosting. On the other hand for sequences that acquire k-space in a block sequential manner a single movement, as long as it doesn't coincide with the acquisition of the centre of k-space, or similarly a drift in position, will cause some blurring but will generally cause less impact through ghosting.

Different segmented sequences have different optimal phase-encoding orders, and therefore will be affected by respiratory motion differently. Generally, to avoid sudden signal amplitude and or phase discontinuities through k-space, which would lead to other artifacts, the Turbo-Spin-Echo (TSE) and conventional gradient echo sequences acquire the data with an interleaved manner, whereas for other reasons the balanced Steady-State Free Precession (SSFP) cine sequences acquire in a block sequential manner. However, it should be noted that the exact acquisition

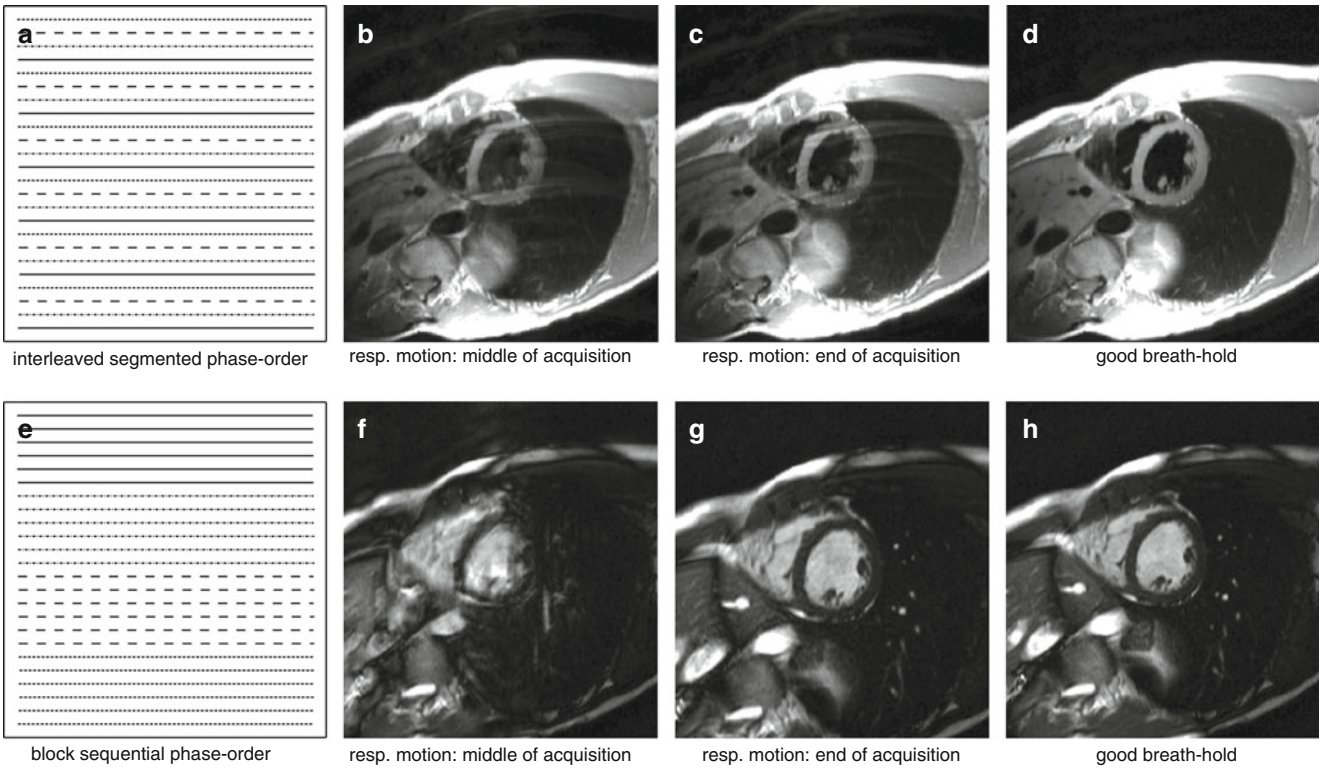

Fig. 7.1 Breathing motion artifacts with two different phase-orders. This figure shows the artifacts caused by changes in respiratory position at different times during a breath-hold acquisition for an interleaved (*top*) and sequential (*bottom*) phase-order. (**a**) Shows an interleaved segmented phase-order (as used in a black blood TSE sequence but reduced to only 24 phase-encode lines for illustration), with 4 segments each with 6 phase-encode lines. Each line-type represents a different cardiac-cycle of data. (**b**) The effects of a respiratory movement in the middle of the acquisition. (**c**) The effects of a respiratory movement at the end of the acquisition. (**d**) A good breath-hold. With interleaved acquisition, respiratory motion at any time during the scan is liable to cause ghosting across the entire phase-encode FOV. (**e**) Shows a block sequential phase-order case (as used in a cine bSSFP sequence and again only 24 phase-encodes for illustration), with 4 segments each with 6 phase-encode lines. Each line-type represents a different cardiac-cycle of data. (**f**) The effects of a respiratory movement in the middle of the acquisition. (**g**) The effects of a respiratory movement at the end of the acquisition. (**h**) A good breath-hold. With a block sequential phase order the central region of k-space is acquired during a certain well defined period, and not spread throughout the whole acquisition window, therefore if no respiratory motion happens during this period, the artifacts are less conspicuous

methods might vary between manufacturers and even for the same manufacturer over time.

To avoid breathing motion artifacts, the total imaging time is kept short, and suitable for a breath-hold. If the patient is unable to hold their breath, the total imaging time needs to be reduced. Possible solutions include end-inspiratory breath-holds risking greater variability, or the use of parallel imaging, although the reduction of SNR in some applications such as Late-Gadolinium Enhancement (LGE) imaging may prohibit this; or the reduction of overall k-space lines acquired, thus reducing phase-encode spatial-resolution. Another solution that may be available is to reduce the temporal-resolution, by increasing the data lines per cardiac cycle and the imaging window of each cardiac-phase. This may have the cost of increasing cardiac motion problems, especially if imaging during rapid cardiac motion stages.

Breathing motion is one of the biggest challenges of MR coronary angiography. During cardiac motion, the coronaries have been shown to shift position from 5 to 20 mm [1], therefore the imaging window is limited to mid-diastole when the heart is relatively still. 3D coronary angiography imaging is performed during free-breathing and uses navigator echo techniques to monitor respiratory motion.

In general if imaging during a breath-hold, a *saturation band* can be positioned over the anterior chest wall to suppress any motion induced ghosting from it, if the breath-hold is imperfect.

Cardiac Motion

Cardiac motion is another source of inter-view motion artifacts. Cardiac motion is mainly a problem in sequences where the data acquisition window includes periods of rapid cardiac motion. This is commonly an issue for first-pass myocardial perfusion imaging, where several images are fully acquired during each heartbeat; therefore image acquisition windows are long and spread across the whole of

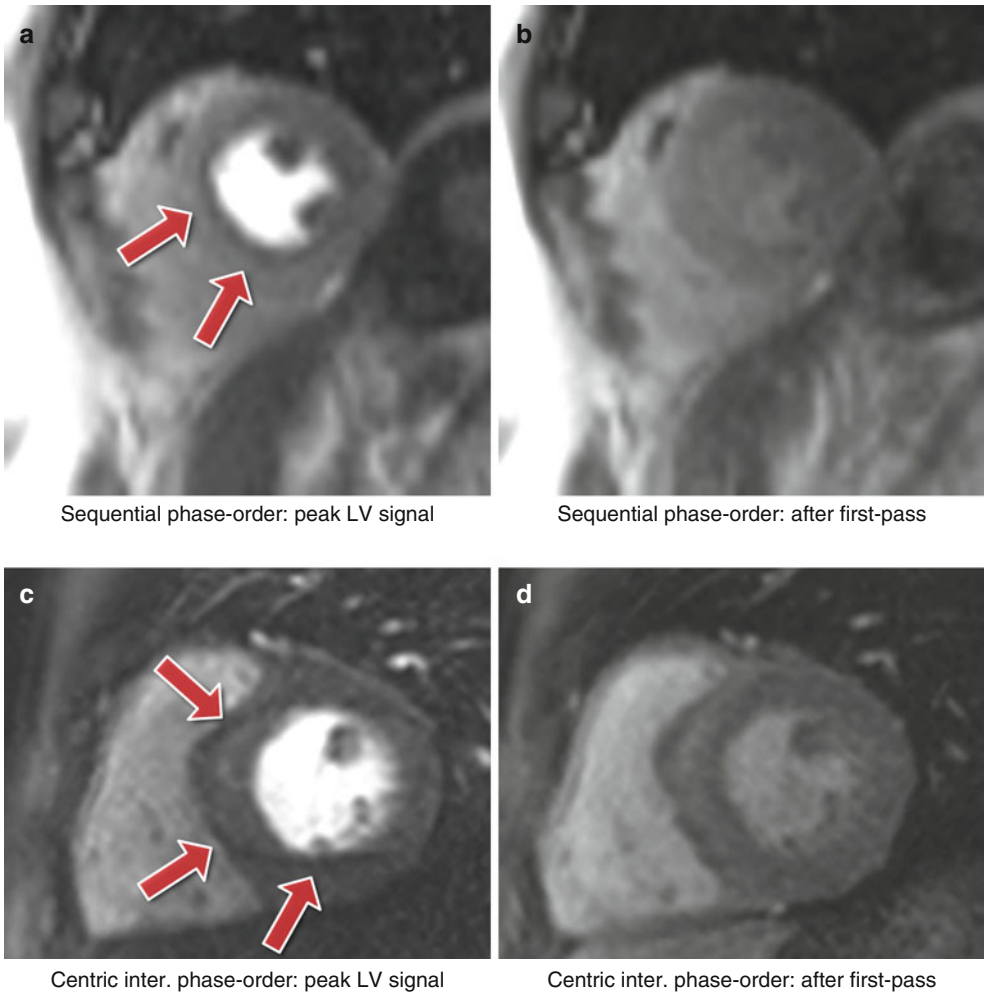

Fig. 7.2 Myocardial perfusion and cardiac motion artifacts for sequential and centric interleaved phase-orders. (**a**) In vivo short-axis image of a perfusion scan with a bSSFP sequence with a sequential phase-order acquisition. A subendocardial dark rim artifact is visible likely to be a superposition of motion and Gibbs ringing artifacts (*arrows*). (**b**) Same as *a* but after first-pass; the contrast between the LV and myocardial signal is reduced and the dark rim artifact is no longer visible. (**c**) In vivo short-axis image of a perfusion scan with an h-EPI sequence with a centric-interleaved phase-order acquisition. A typical motion artifact is visible in the septal wall. This is no longer a subendocardial dark rim as shown in *a,* but ghosting from the endocardial border offset along the phase-encode direction (*arrows*). (**d**) As in *b*, motion artifacts are no longer visible after first-pass due to the reduction of signal contrast between the LV and myocardium (Video 7.1)

the cardiac cycle, including rapid cardiac motion stages. The heart will go through contraction and expansion as different phase-encode lines are acquired; motion happens both in-plane and through-plane, resulting in artifacts. Acquisition windows for one perfusion image at typical in-plane resolution around 2.5 mm are approximately 100 ms for Gradient-Recalled Echo (GRE) and bSSFP sequences and 70 ms for h-EPI, with parallel imaging with an acceleration factor of 2.

For a Cartesian sequential phase-order, as typically employed in GRE and bSSFP sequences, a continuous motion results in banding artifacts next to sharp edges [2], shown in Fig. 7.2a, b. The appearance of these artifacts is similar to *Gibbs ringing* artifacts (described later). Alternatively the hybrid Echo-Planar Imaging (h-EPI) perfusion sequence is commonly used with a centric interleaved phase-order tailored for perfusion, minimising the effective TE, resulting in a dark ghosting of the endocardial border along the phase-encode direction (Fig. 7.2c, d).

For the GRE and bSSFP sequences with a sequential phase-order, motion induced ringing artifacts can be superimposed with Gibbs ringing and possibly mimic real subendocardial perfusion defects during first-pass. The h-EPI sequence is more robust to motion artifacts, not only because it is the fastest of the three sequences, but also because of its different phase-order (centric interleaved); cardiac motion artifacts do not result in subendocardial dark rim artifacts. Whilst the h-EPI sequence is therefore useful to differentiate cardiac motion artifacts this also makes it very sensitive to frequency-offsets as described below.

As the motion ringing magnitude is dependent on the signal difference across the edges, motion artifacts are expected to be problematic during first-pass when there is a large contrast between the LV blood pool and the myocardium.

In general, whatever the k-space acquisition scheme, in order to minimise cardiac motion artifacts it is important to keep the image acquisition time as short as possible in each heartbeat and if possible aim for timings of the heart cycle where the heart is relatively still. Additional approaches include using a fast EPI readout, and/or parallel imaging.

The inversion pulse preparations used in dark-blood imaging or LGE are particularly sensitive to cardiac motion and arrhythmias. For the multiple inversion pulse preparation used in dark-blood imaging, a correct cardiac cycle synchronisation with the readout is important. If during image

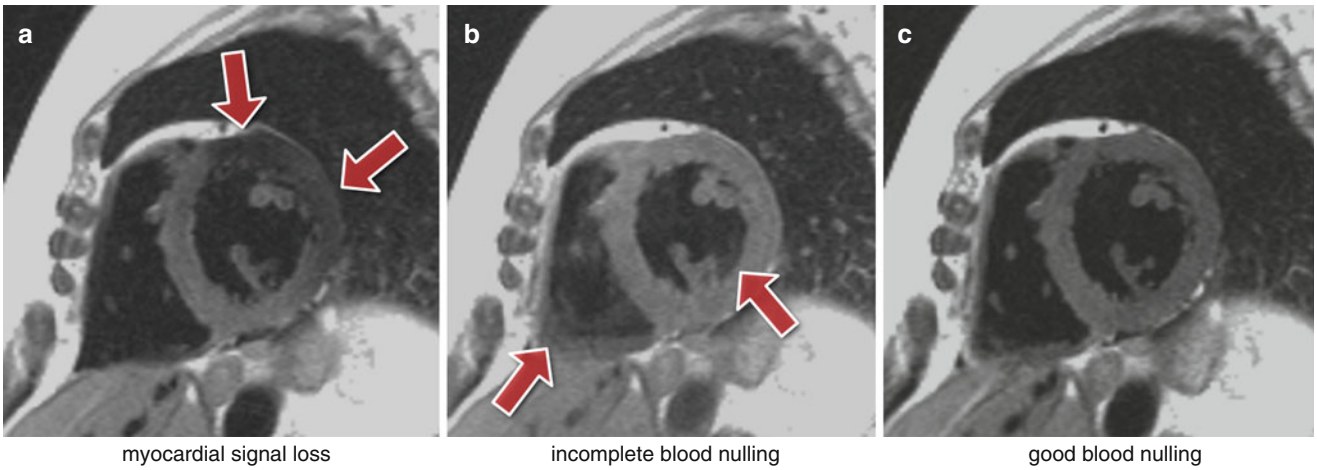

Fig. 7.3 Dark-blood imaging with cardiac motion artifacts. (**a**) Myocardial signal loss (*arrows*) due to incomplete re-inversion of the myocardial magnetisation. (**b**) Partial blood signal (*arrows*) due to incorrect inversion-recovery timing not coinciding exactly with the "null" time of the blood magnetisation. (**c**) Good blood signal nulling, without loss of myocardial signal. In this last example the inversion pulse thickness and timing were optimal for darkening the blood signal

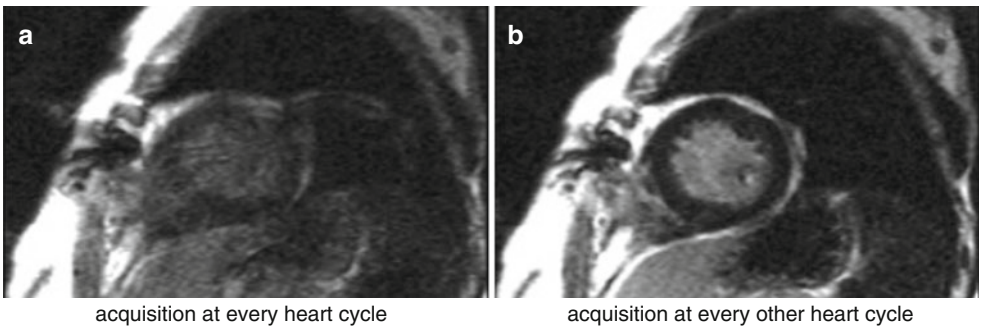

Fig. 7.4 Arrhythmia artifacts in LGE.LGE short-axis image, in a patient with arrhythmia. (**a**) Image acquisition for every heart-cycle. (**b**) Image acquisition for every other heart-cycle. Image quality is improved in *b* by acquiring data at every other heart-cycle only, reducing the contrast inconsistencies between different k-space segments that were created by the irregular heart-rate

acquisition, the heart is not in the same position as when the double-inversion pulses were applied, then the myocardial signal can be affected resulting in myocardial signal loss (Fig. 7.3a). To reduce the potential for this the spatially selective inversion pulse thickness is commonly larger than the image-slice thickness by a factor of 2 or 3. The trade-off is the re-inversion of blood outside the image-slice potentially reducing the blood signal nulling efficiency for slow flow, which may be a factor for patients with an abnormally low cardiac function. Another reason for reduced blood signal nulling efficiency would be an inversion time that was either too long or too short (Fig. 7.3b). Although it is not always possible to change all the parameters required, it is normally possible to adjust the trigger delay and inversion time to change the timings of the preparation and imaging. It should be noted that the terminologies for these timing parameters vary between manufacturers.

Arrhythmias in LGE can lead to poor image quality due to contrast inconsistencies between different k-space segments, due to variations in the TR for the inversion recovery sequence. This leads to different amounts of recovery and therefore different levels of magnetisation before and after the inversion pulse. For this reason data is usually acquired for every other heart-beat, reducing dependency on a regular heart cycle but increasing imaging time (Fig. 7.4). For patients with very fast heart-rates it might be required to trigger every three heart-cycles in order to guarantee good image quality.

Poor cardiac triggering can also result in motion artifacts. Most cardiac imaging techniques require the acquisition of full images or k-space segments at specific cardiac phases, i.e. at specific times after the R-wave. Poor triggering due to patients with arrhythmias or weak ECG signal, or due to magneto-hydrodynamic [3] (generation of an electric field due to ions in blood flowing across the main magnetic field) and/or gradient pulse distortion, can cause effects varying from minor inconsistencies to conspicuous artifacts. For example, poor triggering in myocardial perfusion imaging typically results in slices at different cardiac phases per cycle of the perfusion first-pass series; this may not degrade the image quality of each individual image but it affects the clinical interpretation of first-pass and severely complicates segmentation in quantitative analysis. Triggering problems in cine imaging tend to result in more severe artifacts because each image frame's k-space is segmented across multiple

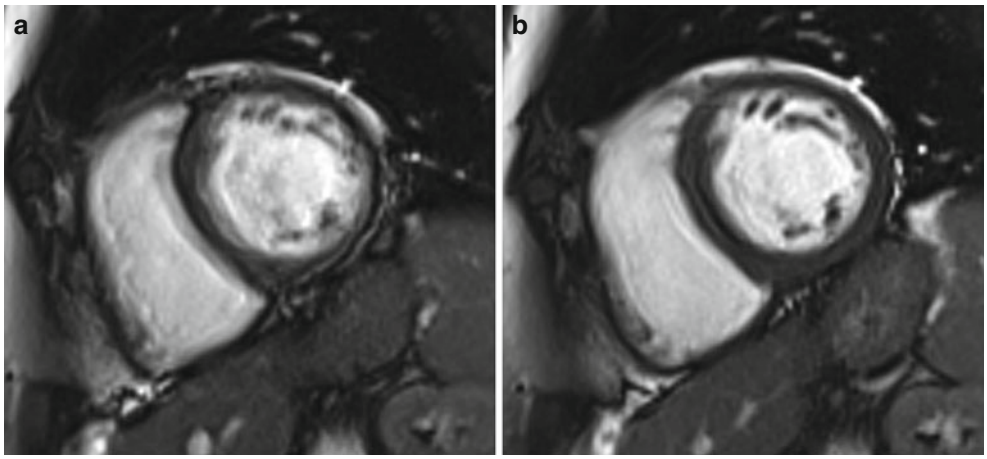

Fig. 7.5 bSSFP cine and arrhythmia. Short-axis bSSFP cine frame imaged twice: (**a**) with significant arrhythmia artifacts and (**b**) with reduced artifacts due to a more stable RR-interval (Video 7.2)

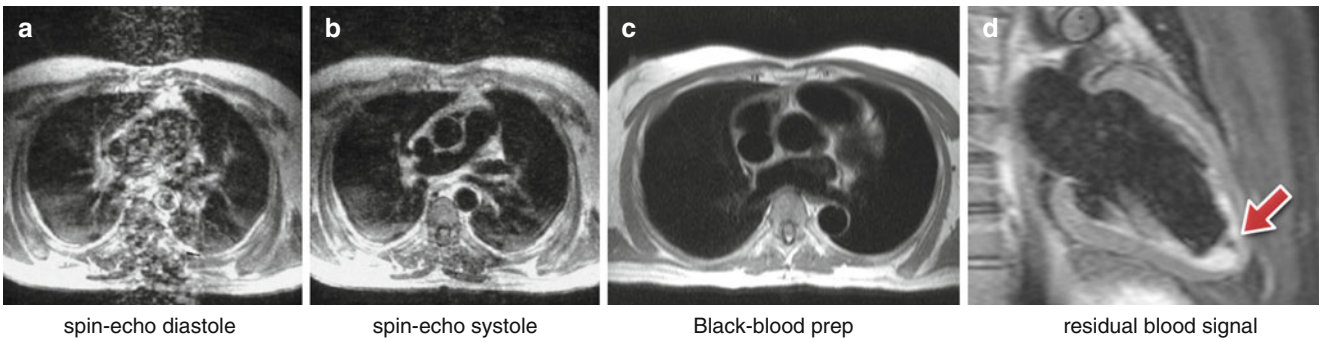

Fig. 7.6 Spin-echo blood flow artifacts. (**a**, **b**) An old example of blood flow artifacts on a conventional spin-echo sequence of a transverse slice through the great vessels above the heart: (**a**) image acquired in diastole, (**b**) image acquired in systole showing reduced flow artifacts due to increased intra-voxel dephasing and time of flight effects. (**c**) Similar transverse plane to *a*-*b*, acquired with a HASTE sequence in diastole. The introduction of faster segmented acquisitions with black blood preparation avoids flow artifacts in diastole; multiple spin-echo sequences (HASTE, FSE) are generally reliable only in diastasis. (**d**) Dark-blood prepared FSE image (with STIR fat suppression) shows residual slowly moving blood signal (*arrow*) that was re-inverted by the double inversion preparation pulse and did not wash out between preparation and imaging

heart-cycles. Mis-triggers causing jumps in TR and or heart-cycle variations will create inconsistencies between k-space segments, thus leading to noticeable cardiac motion artifacts (Fig. 7.5). If ECG triggering quality is low, alternatives can be used such as pulse oximeters, although care must be taken with the fact that the pulse cycle is delayed relative to the heart-cycle and not as well defined, thus reducing timing precision. More recently real-time imaging strategies have been developed where the requirement of ECG triggering and/or breath-holding are relaxed [4].

Blood Flow

Flowing blood has historically been a source of artifacts on CMR images. For conventional sequences the movement of blood results in a signal phase shift related to the velocity of the blood flow. This would not cause a major problem if the blood flow was exactly the same on each successive cardiac cycle of the scan; however, this is not usually the case and the result is that this changing velocity related phase shift will add to and corrupt the spatial phase encoding in such a way that the Fourier transformation will interpret the blood signal as coming from a range of locations spread across the image along the phase-encode direction. To avoid this problem in the early days of CMR for spin-echo acquisitions the images were often acquired in systole, when two factors combined to cause a loss of blood signal. Firstly, the blood flow was fast causing increased phase shifts leading to a broad phase distribution at a voxel scale known as intra-voxel phase dispersion, and secondly time-of-flight effects meant that the same blood was not excited by both the slice selective 90° and 180° pulses (Fig. 7.6a, b). With the introduction of faster segmented acquisitions of spin-echo images with double inversion blood signal nulling, this problem was largely removed (Fig. 7.6c), although residual static blood at ventricular trabeculations is commonly visible as a white layer in the left ventricle (Fig. 7.6d).

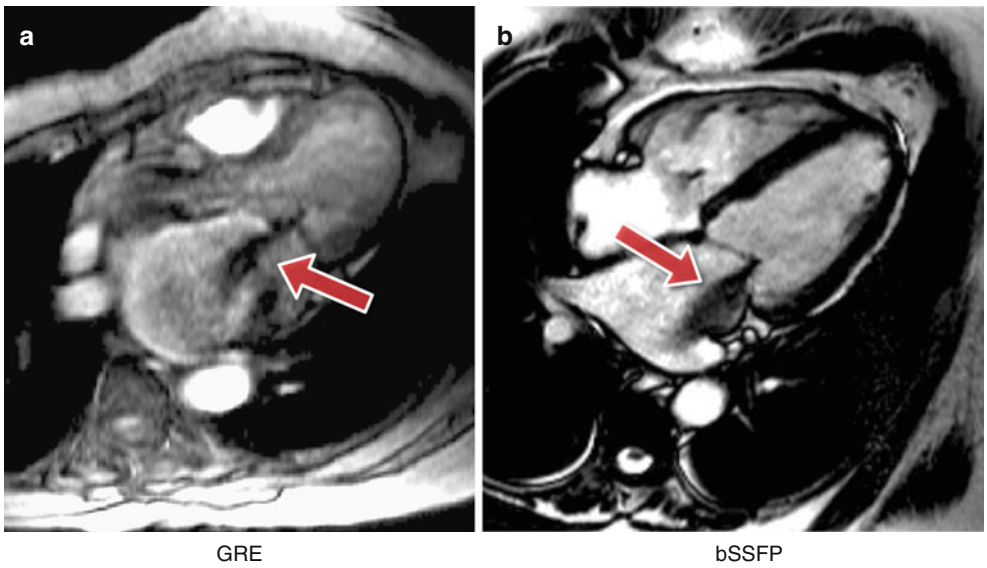

Fig. 7.7 Complex flow signal loss. Two examples of a systolic frame of an horizontal long axis cine acquisition from two different patients with insufficient mitral valves: (**a**) GRE, (**b**) bSSFP. The jet of signal loss caused by complex flows in the left atrium suggests mitral valve regurgitation (*arrows*)

For gradient-echo acquisitions in the early days the problem was largely removed by the introduction of velocity or flow compensation to null velocity related phase shifts. With the introduction of faster gradient performance and shorter TE's and consequently greatly reduced velocity related phase shifts, the potential for these artifacts has been reduced. Nonetheless velocity compensation remains an option to minimise the problem. However, as a consequence of some cardiovascular diseases, the blood flow often becomes much more complex and turbulent and contains higher orders of motion than simple velocity, (acceleration, jerk, etc.). These higher orders of flow motion can introduce phase shifts even to a velocity compensated sequence and the spatial scale of this motion is such that this can also lead to significant phase dispersion. This intra-voxel phase dispersion effect is dependent on the TE. Although this signal loss artifact has been found useful by some to assess the severity and form of defective heart valves (Fig. 7.7) it should be used with caution as the area of signal loss may not be directly related to the severity of the valve stenosis.

Gibbs Ringing

Gibbs ringing, also known as a truncation artifact, is present in every unfiltered MRI image and results from the fact that there is only enough time to acquire a finite region of k-space for each image. When the sampled signal is truncated at the k-space edge and then this k-space is inverse Fourier transformed into the image, ringing will unavoidably be present at high-contrast sharp edges of structures on the image. The ringing is a known mathematical limitation of the Fourier transform.

The 2 pixels both sides of and closest to the edge will show a maximal undershoot and overshoot of the true signal. The magnitude of the under/overshoot can be shown mathematically to be approximately 9 % of the edge signal difference; the ringing magnitude is thus dependent on the signal difference at the edge, the higher the signal discontinuity the higher the under/overshoot (Fig. 7.8a, b). Gibbs ringing also scales with pixel size, i.e. the higher the spatial-resolution the thinner the ringing, but the under/overshoot magnitude does not change with spatial-resolution. The ringing visibility is also dependent on the edge position inside the pixel [5] (unless zero-filling is applied in k-space for interpolation, making Gibbs more consistent).

Gibbs ringing is present in all unfiltered MRI images, but it is especially problematic in certain applications such as myocardial first-pass perfusion studies where the spatial-resolution is low to reduce acquisition time. Gibbs ringing can mimic a real subendocardial perfusion defect during first-pass due to the large signal discontinuity between the bright LV blood pool and the darker myocardium [6].

One way of reducing Gibbs artifacts is by filtering the k-space data of the image, a process usually known as apodization. Hamming and Hann filters are commonly used in image and signal processing to reduce Gibbs ringing artifacts, although at the penalty of reducing spatial-resolution. Due to the image constraints of most cardiac imaging protocols, any further loss in spatial-resolution may affect diagnostic confidence and is therefore seldom used. It is then perhaps better for clinical diagnosis and image interpretation to be performed with some understanding of the characteristics of these artifacts and can discriminate between them and true perfusion defects (which is sometimes ambiguous, especially for mild perfusion defects). The access to k-space filtering options in the scanner's protocol may vary for different manufacturers.

Increasing spatial-resolution does not reduce the Gibbs ringing magnitude but it will make it less conspicuous due its

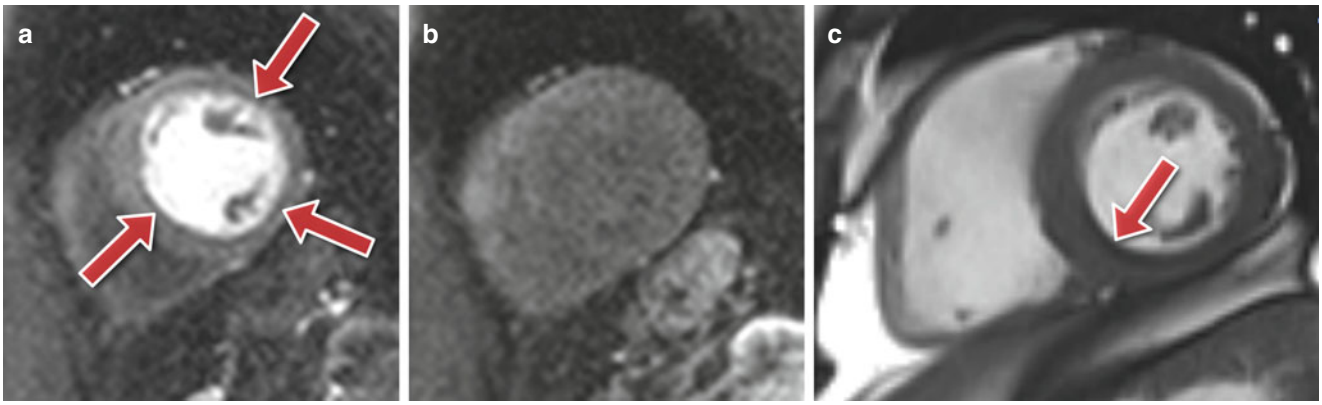

Fig. 7.8 Gibbs ringing. (**a**, **b**) In vivo short-axis first-pass perfusion example: (**a**) circumferential Gibbs ringing during the first-pass of contrast (*arrows*); (**b**) the same short-axis plane after the first-pass when Gibbs ringing is no longer noticeable. (**c**) Example of Gibbs ringing in a short-axis frame of a bSSFP cine (*arrow*)

property of scaling with pixel size. Unfortunately in many cases it is not possible to increase the resolution as this would require increased time, which might not be available. Additionally, other sources of artifacts such as cardiac motion could be worsened. However, as techniques such as parallel imaging and other image acceleration methods improve they can be used to increase spatial-resolution without increasing imaging time [7–9], provided that loss of SNR and other consequences of acceleration are acceptable.

Even though this section focused on myocardial perfusion, Gibbs ringing is visible at any sharp edge, and therefore it could affect many other cardiac applications. For example, Fig. 7.8c shows an example of suspected Gibbs ringing in a short-axis frame of a bSSFP cine.

Aliasing or Wraparound Artifacts

One of the most basic artifacts commonly seen in MRI is the phase-encode field-of-view (FOV) *wraparound* artifact also known as *aliasing*. This artifact occurs whenever the size of the object being imaged exceeds the FOV in the phase-encode direction; the outside regions are wrapped into the opposite edge of the FOV. This is due to the failing of the Nyquist sampling requirements of the k-space signal for parts of the object outside the FOV. Aliasing is prevented along the frequency-encode direction either by filtering the frequencies above a limit determined by the Nyquist sampling requirement; or by signal oversampling, i.e. sampling more points in k-space than the ones prescribed by the protocol such that the FOV along the frequency-encode direction is bigger than that actually displayed on the image. The same technique cannot be used along the phase-encode direction without increasing the time of imaging. Therefore this type of artifact is common along the phase-encode direction and also along the slice direction in a 3D acquisition. Figure 7.9b illustrates the chemical shift effect described below but also very nicely illustrates aliasing of patient's arms into his chest.

Due to the need of large FOVs to cover the chest, aliasing is a common problem. If the region of interest is small, for example the heart only, then some wraparound can be acceptable as long as it does not superimpose on the heart. This keeps imaging time short without sacrificing diagnosis and experienced technologists commonly make careful use of this approach. Saturation bands can also be used to suppress the signal of the regions outside the FOV in sequences where the signal used for the acquisition is excited only once and immediately after the saturation, such as in the 90° excitation of a multiple spin-echo (FSE or TSE) sequence.

We have discussed aliasing artifacts in this section for Cartesian sampling only. Aliasing and undersampling artifacts are discussed further in section "Artifacts specific to advanced cardiac imaging methods", particularly regarding non-Cartesian trajectories and parallel imaging.

Chemical Shift

The resonance frequency of water and fat differs by approximately 210 Hz at 1.5 T (420 Hz at 3 T), which causes a number of effects. Firstly it causes a *misregistration* between fat and water based tissues along the frequency-encode direction and more so along the perpendicular phase blip direction for EPI sequences. Secondly, it will result in a slice excitation offset between water and fat. Finally, for gradient-echo sequences only, a possible pixel cancellation effect at water-fat boundaries can occur.

The misregistration in pixels along the frequency direction results from the fact that fat and water that are

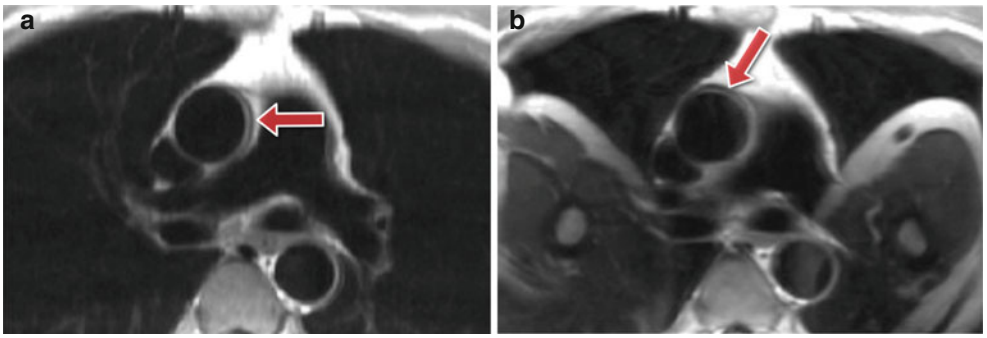

Fig. 7.9 TSE chemical shift artifacts. (**a**, **b**) TSE image of a transverse plane through the great vessels above the heart, illustrating chemical shift artifacts between the aortic wall and surrounding fat: (**a**) horizontal frequency-encode, (**b**) vertical frequency-encode. Artifacts are visible in the aortic wall along the frequency-encode direction (*arrows*). This artifact can potentially be misdiagnosed as an aortic dissection in some cases. On image *b* with the frequency-encode direction swapped from *a*, wraparound artifacts of the patient's arms into the chest are also visible

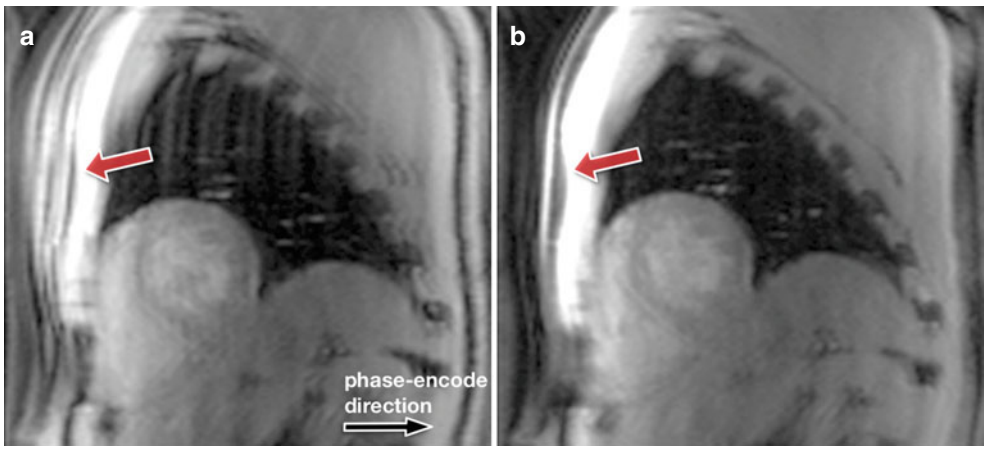

Fig. 7.10 h-EPI chemical shift artifact. Short-axis images acquired with a centric interleaved h-EPI sequence with fat-saturation preparation turned off (**a**) and on (**b**). When there is no fat-saturation preparation, the fat signal in the chest wall is visible, displaced approximately 4 pixels in both directions (*arrows*). When fat saturation pulses are used, the fat signal in the chest wall is efficiently suppressed (*arrow*)

physically in the same position have different resonance frequencies, which will result in the frequency encoding process separating them on the reconstructed image. The distance of separation will depend on the receiver bandwidth. For example, if the bandwidth was 105 Hz/pixel then at 1.5 T their separation of 210 Hz would equate to 2 pixels on the reconstructed image. If the bandwidth was doubled to 210 Hz/pixel then the separation would be halved to 1 pixel. Increasing the bandwidth thus reduces the chemical shift effect; however, this has to be balanced against the loss of SNR. For most cardiac applications, the need of rapid sampling requires large bandwidths, so misregistration along the frequency-encode direction is relatively negligible. However, for TSE sequences where longer readouts with lower bandwidths can be used, it is possible to see the effect (Fig. 7.9).

As mentioned above, for an EPI readout misregistration can be a problem and can cause a considerable shift of the fat signal along the phase-encode direction relative to the water signal. For a single shot EPI acquisition, the shift can be several pixels and for a typical perfusion h-EPI sequence a chemical shift of a pixel or two is typical. Where centric phase encoding is used, as is often the case, the shift is doubled and split into two opposite directions producing a complicated artifact when fat saturation is not applied correctly (Fig. 7.10). Using a small number of echoes per readout train or fat saturation pulses are common techniques to reduce chemical shift artifacts in EPI.

Another important artifact resulting from the chemical shift and sometimes referred to as the *Indian ink* artifact, is the pixel cancellation at boundaries between fat and water based tissues. This occurs with gradient-echo sequences and is TE dependent such that the maximum cancellation occurs when fat-water signals are completely out of phase, which first occurs at a TE of approximately 2.4 ms for 1.5 T. This is often prominent on bSSFP images where the TR has to be kept short enough to minimise the sensitivity of the sequence to field inhomogeneities and this generally leads to a TE in the order of 2 ms (Fig. 7.11). When imaging the coronaries, the signal cancellation artifacts can reduce the apparent diameter of the coronary arteries if fat signal is not properly suppressed.

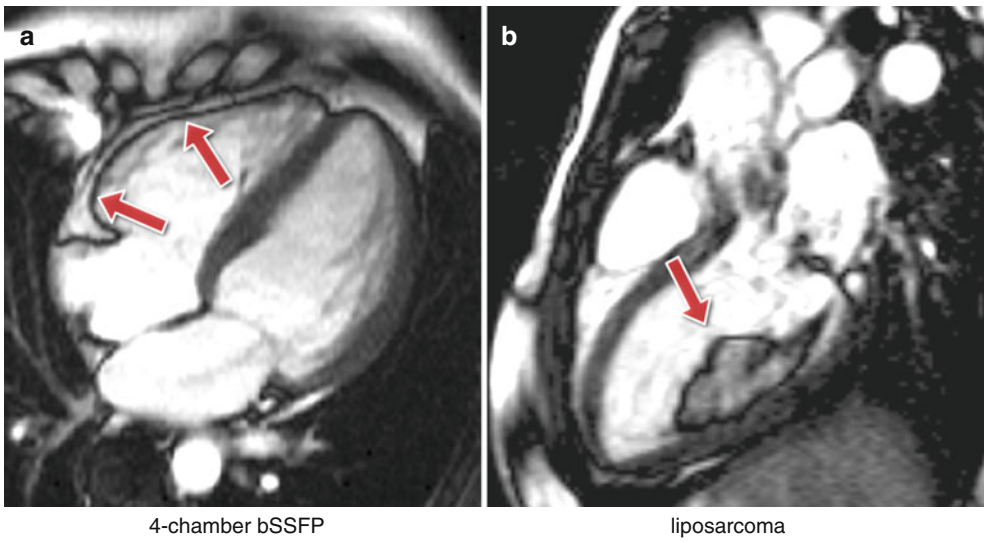

Fig. 7.11 b-SSFP Fat-water signal cancellation. At TEs of approximately 2.4 ms at 1.5 T (1.2 ms at 3 T), the fat and water spins are out of phase and the resulting signal is reduced. (**a**) Fat water cancellation artifact around the right ventricular wall (*arrows*) on a long-axis cine. (**b**) The same artifact around a liposarcoma in the left ventricle (*arrow*)

B_0-Field Inhomogeneities

The magnetic field is never completely homogeneous over the volume of the heart. It is possible to correct low spatial-order variations by obtaining 3D field plots and calculating the required shim currents usually to second order; however, more localised (high-order) field variations will remain due to the magnetic field susceptibility variations around the heart.

Most tissues are *diamagnetic*, i.e. create a magnetic field that slightly opposes the applied magnetic field. It is important to understand that this arises from their electronic ("Lenz") diamagnetism, which is much larger than the nuclear magnetisation we employ for MRI. The differences in diamagnetism cause distortion of the main field at interfaces between tissues, and particularly those between tissue and air such as between the heart and lungs. These B_0 field inhomogeneities cause resonance frequency offsets, where the local resonance frequency deviates from the scanner's reference frequency, leading to off-resonance effects. Depending on the local geometry, and the sequence being used, this field distortion may sometimes be more intense causing artifacts such as signal loss or spatial distortion.

In CMR the sequences with the highest sensitivity to magnetic field inhomogeneities are the bSSFP sequence and sequences that employ rapid k-space acquisition techniques such as EPI and Spiral. The spin-echo sequence is relatively insensitive whilst the conventional gradient-echo sequence sensitivity increases largely with its TE parameter. Figure 7.12 illustrates the difference between a TE of 2 and 10 ms for distortion, signal loss, and phase shift caused by susceptibility variations around a pulmonary vessel and around the apex of the right ventricle on a GRE sequence.

Figure 7.13 illustrates an example where a patient with an insertable cardiac monitor has been scanned with both bSSFP and HASTE sequences. The bSSFP image shows signal loss and banding artifacts in the region proximal to the device due to magnetic field distortions, while the HASTE sequence is less sensitive. Many other medical devices are also a source of susceptibility artifacts by distorting the magnetic field (Fig. 7.14). Figure 7.15 shows an example of a patient with an aortic stent. When imaged with GRE 3D or bSSFP sequences, the stent causes not only localised main field inhomogeneities and signal loss but also an RF shielding effect within the stent, as elucidated by Fig. 7.15b.

B_0 inhomogeneity artifacts are very distinct and can be very severe for the bSSFP sequence [10]. The steady-state signal response to B_0 inhomogeneity remains approximately constant for small frequency-offsets, but drops down to near zero to form dark bands at regularly-spaced frequency offsets. The more inhomogeneous the magnetic field, the larger the frequency distribution in the image volume and the more black bands will appear. The frequency separation between regions with no signal is inversely proportional to the TR of the sequence; thus, reducing the TR reduces the number of artifacts observed.

Localised field inhomogeneities due to susceptibility differences in the locality of the cardiac veins [11]; and at tissue-air interfaces such as the heart-lung interface [12], or adjacent to air pockets [13] (in the bowel, stomach, and colon for example), introduce banding type artifacts on bSSFP images that can confuse the image interpretation. These signal loss artifacts should not be confused with intravoxel dephasing which is caused very differently. In this sequence, blood flow can also create artifacts in the presence of field inhomogeneities. Moving spins can exhibit signal variations and loss due to the breakdown of the steady-state signal

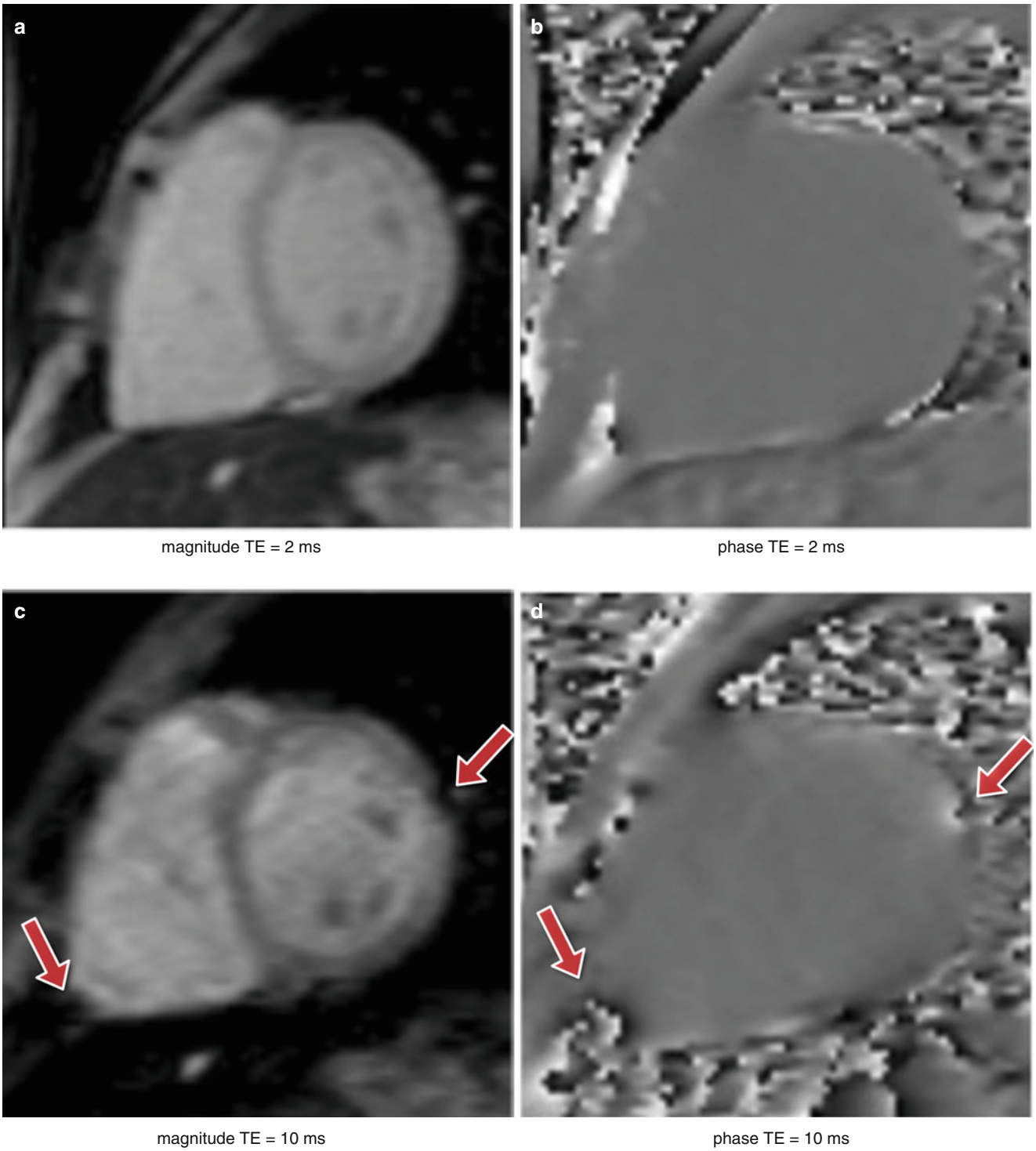

Fig. 7.12 GRE B_0 inhomogeneities at different TEs. Short-axis images acquired with a GRE sequence at two different TEs (**a**, **b**) 2 ms and (**c**, **d**) 10 ms. Both magnitude and phase images are shown. The *arrows* point at two local field distortions (RV apex of the heart and in the proximity of a pulmonary vessel) that generate signal loss in the surrounding region as TE becomes larger

[14, 15]. These can occur due to in-plane flow moving through an off-resonance region, but also for through-plane flow leaving the image plane into such a region. Dark bands and signal variation artifacts are shown in Fig. 7.16. If such artifacts affect an image then it is possible to move and/or suppress these by reacquiring with a slight frequency offset (≈50 Hz) of the scanner reference-frequency. It should be recognised, however, that as one black band moves out of the

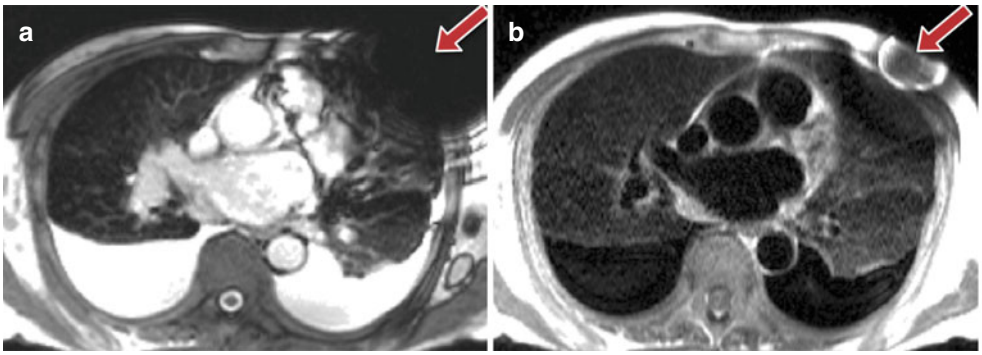

Fig. 7.13 B_0 inhomogeneities and medical devices. Artifacts caused by an insertable cardiac monitor in a transverse plane through the great vessels above the heart: (**a**) image acquired with a bSSFP sequence with visible signal loss and banding artifacts (*arrow*), (**b**) image acquired with a HASTE sequence with less pronounced artifacts (*arrow*)

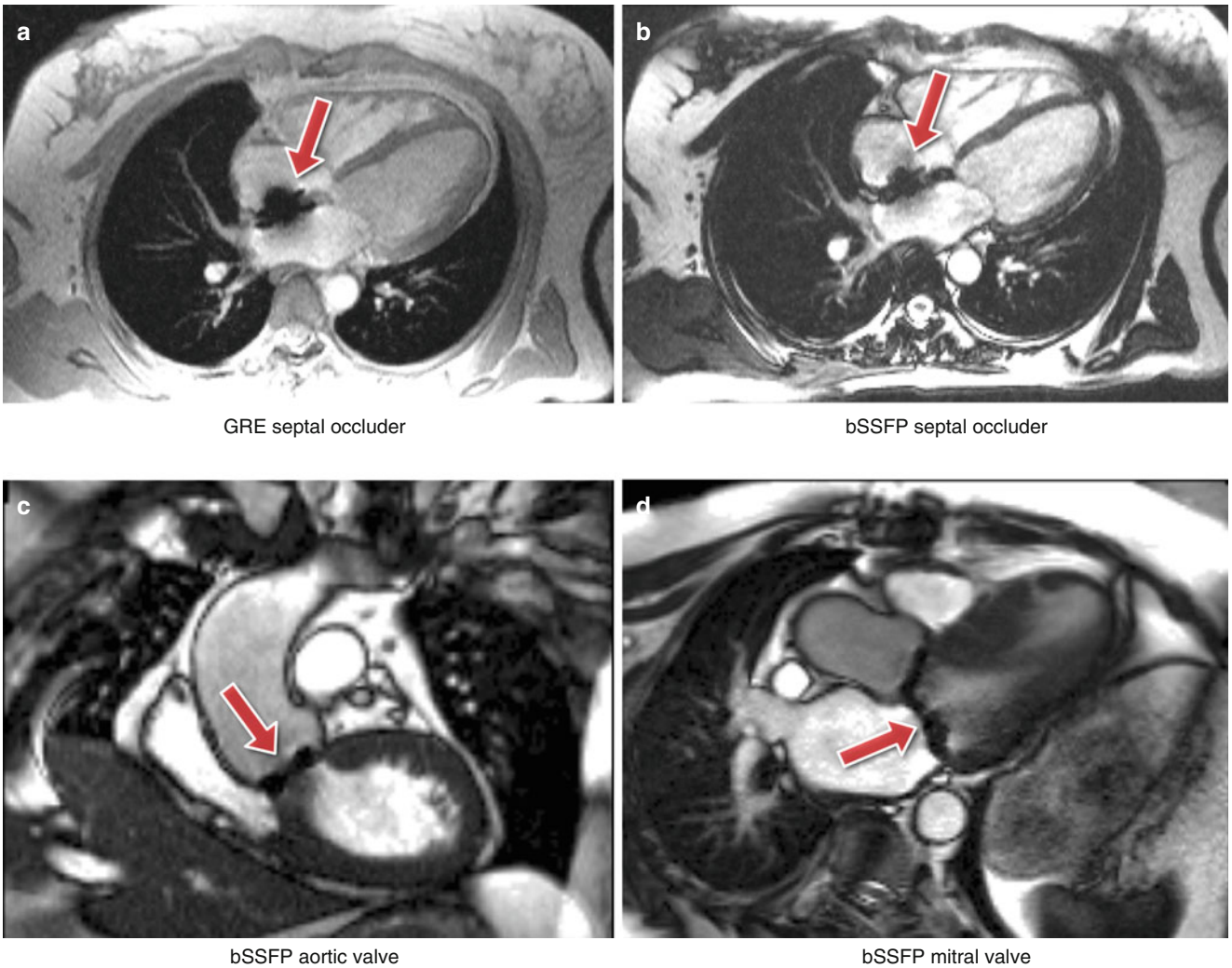

Fig. 7.14 B_0 inhomogeneities and medical devices II. (**a**, **b**) Four-chamber view acquired with GRE and bSSFP sequences respectively. The *arrows* point to signal loss caused by a septal occluder. (**c**, **d**) bSSFP image planes containing localised signal loss (*arrows*) caused by bileaflet aortic and mitral valve replacements respectively

heart then another may be moving in from the other side (Fig. 7.16d). It is also sometimes crucial with such localised adjustments to understand that they should not be confined to the slice thickness. In the situation where through-plane flow or motion is large, then the shim adjustment should include sufficient distance perpendicular to the slice-plane.

Field inhomogeneities are also an important source of artifacts for the less widely-used EPI sequences. Sequences with an EPI readout tend to be used in a hybrid approach (h-EPI), in order to keep the readout train reasonably short, thus minimising blurring, ghosting, image distortion, and chemical shift artifacts. h-EPI sequences are commonly used

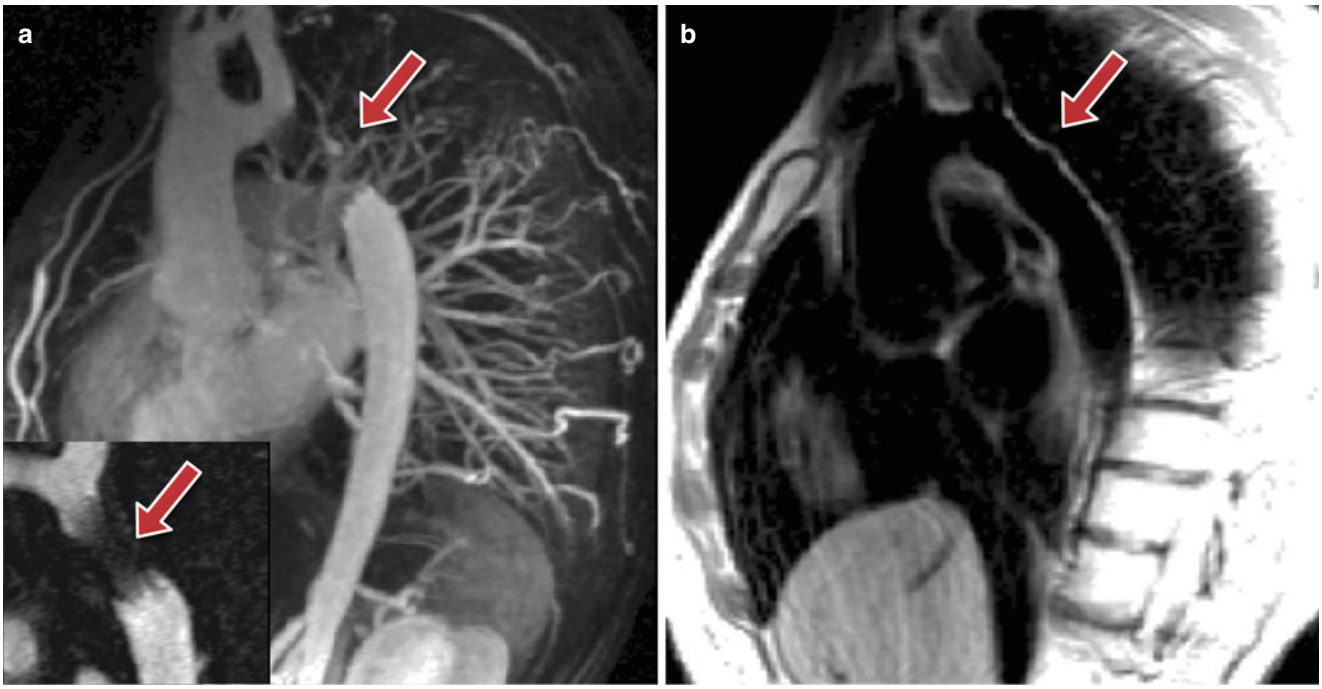

Fig. 7.15 B_0 inhomogeneities and medical devices III. (**a**) 3D GRE contrast-angiography maximum intensity projection reconstruction image showing signal loss in the descending aorta due to an aortic stent (*arrow*); the *bottom left corner* shows *a* bSSFP image plane containing the aortic stent also showing signal loss in the same region (*arrow*). The signal void inside the stent is likely to be due to lack of RF penetration through the stent wall. (**b**) Spin-echo black-blood image also in a plane containing the aortic stent. The aortic wall outside the stent is clearly seen (*arrow*)

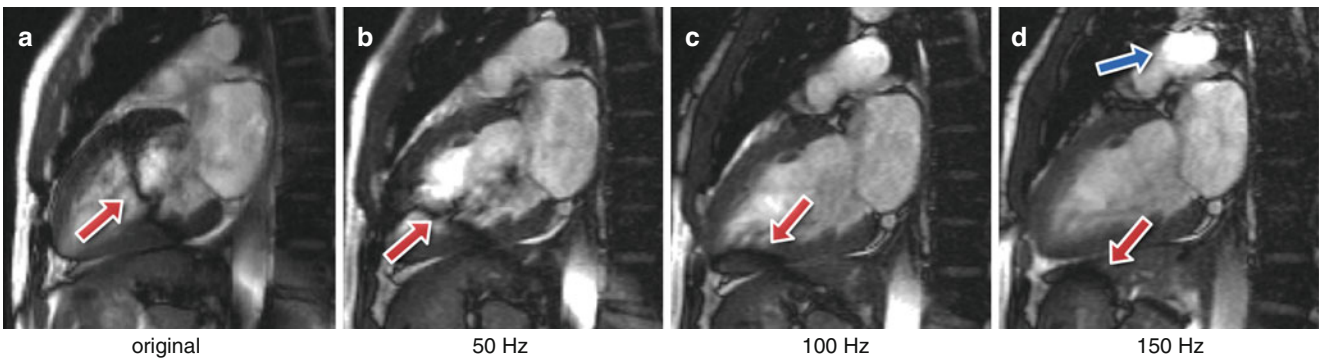

Fig. 7.16 bSSFP and B_0 inhomogeneities: reference frequency. (**a**–**d**) Series of vertical long axis bSSFP images acquired with different reference frequency offsets: original (0 Hz), 50 Hz, 100 Hz, and 150 Hz. Black band and flow artifacts through the ventricle are shown (*arrows*). As the frequency is adjusted, the artifacts are shifted away from the heart. Image *d* shows a new flow artifact approaching the heart from the top (*blue arrow*). The approaching frequency-offset causes the blood signal to be hyperintense in the region

with an interleaved phase-order, where frequency offsets will introduce phase variations in a stepwise fashion, which can lead to artifacts such as blurring and ghosting. Magnetic field inhomogeneities caused by the arrival of a strong paramagnetic susceptibility contrast agent in the heart are commonly attributed as a possible mechanism for dark rim artifacts in myocardial perfusion imaging. The frequency offsets introduced in the myocardium by the first-pass of a Gadolinium-based contrast agent have been measured at rest and shown to be insignificant for intra-voxel signal dephasing in the myocardium at 1.5 T [16], although when combined with other sources of field inhomogeneities or reference frequency-offsets it might produce artifacts such as signal loss or image degradation. The perfusion tailored h-EPI sequence has a centric interleaved phase-order, which makes it very sensitive to frequency-offsets [17], resulting in ghosting and splitting of the image along the phase-encode direction due to its centric sampling trajectory (Fig. 7.17).

In general to minimise B_0-inhomogeneities careful shimming and especially localised scanner frequency adjustments are advised prior to imaging.

Inversion Pulse Ghosting

One artifact that affects any segmented acquisition with an inversion pulse, such as LGE imaging and STIR sequences, is the ghosting of fluids with a long T_1. The long T_1 produces a signal oscillation during its approach to the steady-state, with the signal inverting the magnetisation sign in alternate cycles of the acquired data, resulting in ghosts along the phase-encode direction.

Ghosting of the cerebrospinal fluid (CSF), which has a very long T_1, is common in LGE and STIR black-blood studies. This is usually suppressed by applying a spatial saturation band (Fig. 7.18a–d). A possible example of the same ghosting mechanism of a pleural effusion in a STIR sequence is also shown in Fig. 7.18e.

Fig. 7.17 h-EPI perfusion and B_0 inhomogeneities. Three frames during contrast first-pass perfusion imaging in a basal short-axis plane acquired with an h-EPI sequence. This example shows severe frequency-offsets which result in blurring and ghosting (*arrows*) along the phase encode direction (*vertical*) with this sequence. This example is extreme and uncommon, although blurring of the myocardial wall along the phase-encode direction is believed to be a more common event in first-pass perfusion with this particular sequence

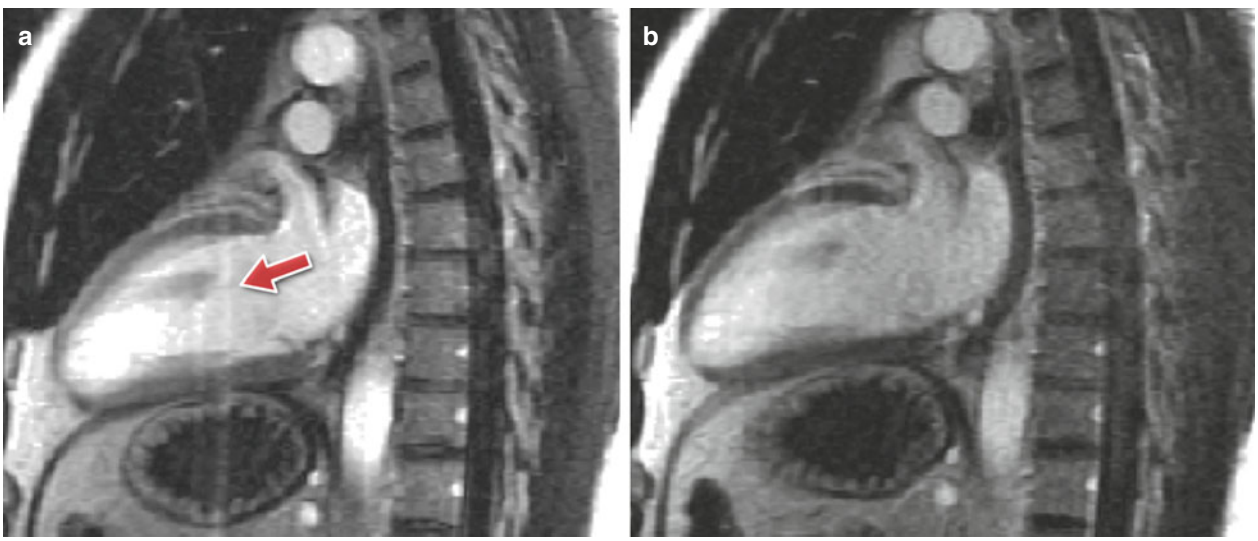

Fig. 7.18 CSF and pleural effusion ghosting. (**a**, **b**) Long-axis LGE image: (**a**) CSF ghosting is visible in the heart (*arrow*), (**b**) CSF ghosting suppressed by a saturation band placed over the spinal canal. In this example the spatial location of the saturation is not very clear, this is presumably because of the timing of the spatial saturation that cannot immediately precede the imaging k-space centre, and the Mz recovery of other tissues due to gadolinium shortened T_1. However, the T_1 of CSF remains very long, which means that this stays well saturated. (**c**, **d**) dark-blood (double-inversion-prepared) and STIR transverse TSE image: (**c**) CSF ghost visible in the RV (*arrows*), (**d**) CSF ghosting suppressed by saturation band placed over the spine (*arrow*). (**e**) Ghosting of the fluid in the pleural layers (pleural effusion) (*arrows*) in part due to its long T_1. Pulsatility effects may also be present, contributing to the ghosting

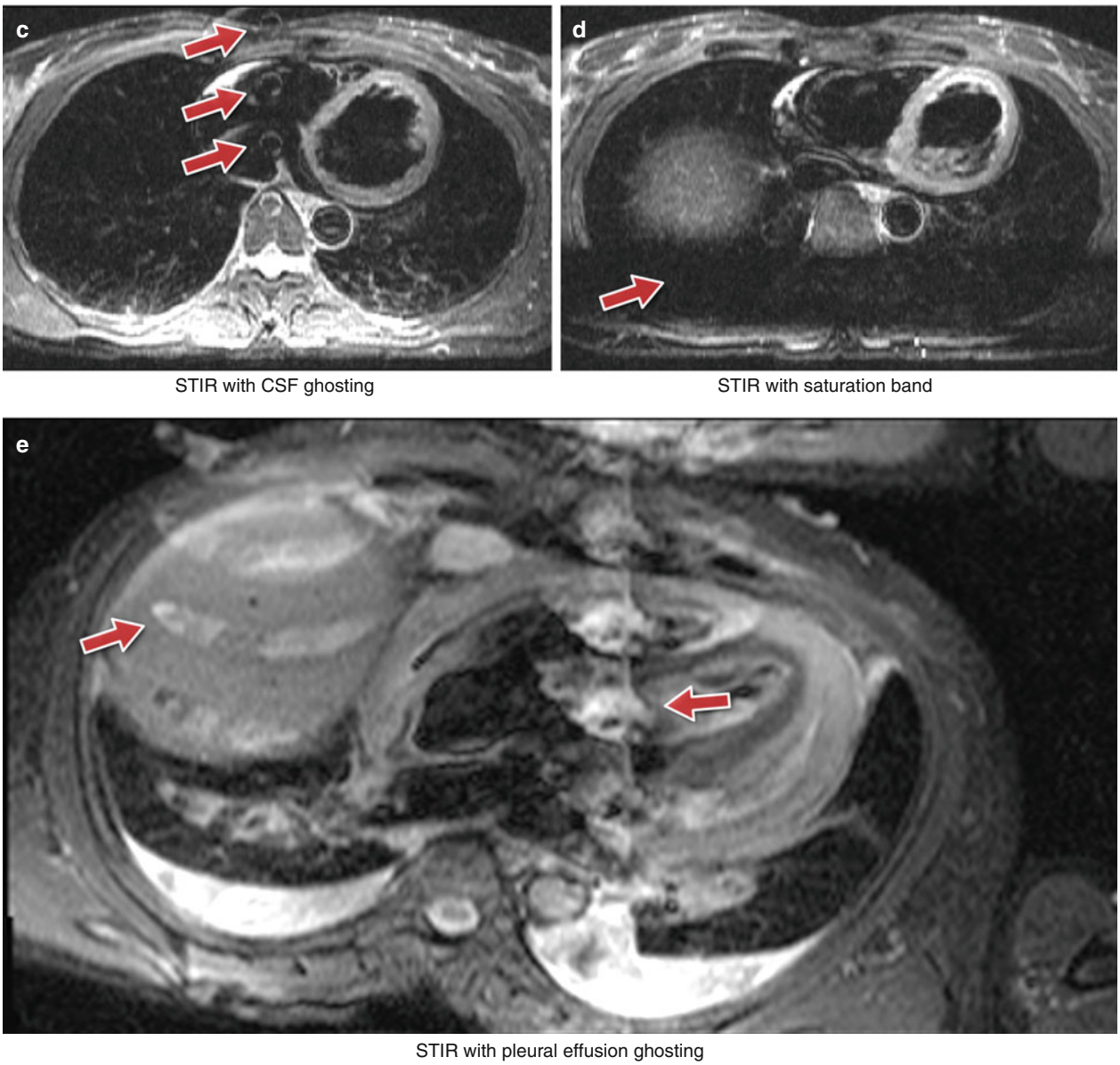

Fig. 7.18 (continued)

Artifacts Specific to Advanced Cardiac Imaging Methods

Methods of more efficiently acquiring the MR data are of particular interest to CMR because of the compromises that have to be made to acquire image data in a short time, often restricted to a fraction of one cardiac cycle or fractions of multiple cardiac cycles within a breath-hold. Methods such as non-Cartesian sampling, parallel imaging, and partial-Fourier have been introduced to accelerate the acquisition. Although each of these methods may work well a proportion of the time and in particular if extra care is taken to set up the scan, they all tend to reduce the imaging robustness and tend to produce artifacts on images and or produce artifactual measurements.

Parallel imaging accelerates image acquisition which has the potential to reduce some problems. For example, although parallel imaging introduces an SNR penalty, it may also be employed to shorten the readout time of an EPI sequence reducing distortions caused by field inhomogeneities, decreasing blurring due to T_2* and or T_2 decay and reducing sensitivity to motion. However, parallel imaging artifacts may appear if inaccurate coil sensitivity maps are acquired, for example due to respiratory motion, where errors will result in reconstruction artifacts (Fig. 7.19).

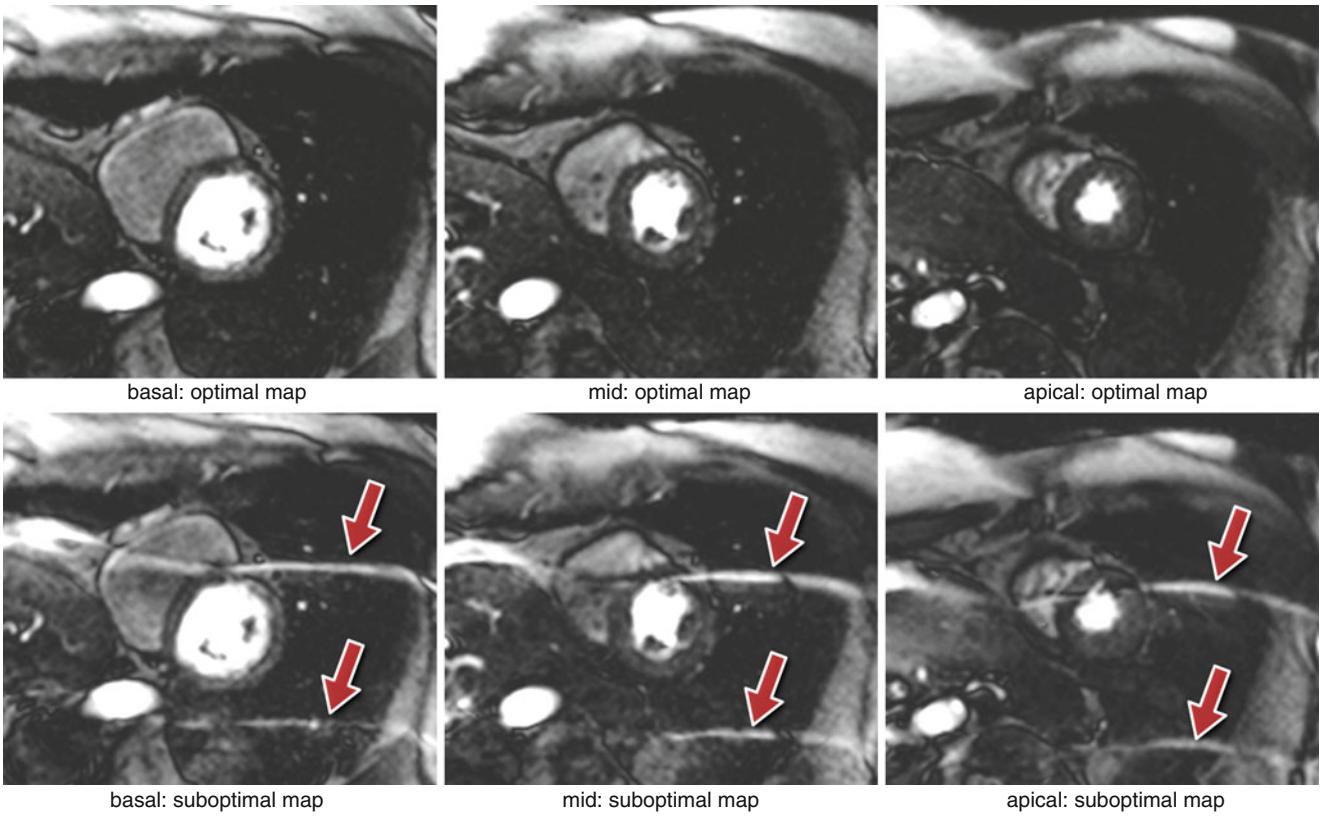

Fig. 7.19 SENSE with aliasing artifact due to respiratory motion. Three short-axis slices during first-pass perfusion, reconstructed with two different coil sensitivity maps (acquisition with a bSSFP sequence and SENSE with an acceleration factor of 4; zoomed images are shown). The three slices on *top* were reconstructed with the optimal coil sensitivity map, i.e. the coil sensitivity map acquired in the same respiratory position as the perfusion images. On the *bottom* the same perfusion images were reconstructed with a coil sensitivity map that was acquired in a different respiratory stage from the perfusion images. The reconstruction is corrupted with aliasing artifacts (*arrows*) due to inconsistencies between the coil sensitivity map and the undersampled perfusion data (Video 7.3)

Sequences with non-Cartesian forms of k-space coverage such as radial and spiral have also been used to image the heart [18–20]. Artifacts discussed earlier can have very different characteristics when compared to the more conventional Cartesian methods.

Radial and spiral k-space acquisitions are generally thought of as being less sensitive to motion. Radial sequences tend to oversample the centre of k-space and this tends to reduce the visibility of breathing artifacts [21]. For a radial acquisition instead of ghosting in the phase-encode direction as seen with Cartesian sampling, respiratory motion results in streaking artifacts propagating from the moving object, perpendicular to the motion direction. For spiral sequences, motion artifacts tend to take the form of swirls and depending on the imaging region of interest these can be less of a problem than phase-encode ghosts.

Non-Cartesian approaches with long (>15 ms at 1.5 T) acquisitions after each RF pulse are highly sensitive to field inhomogeneities, where generally off-resonance and chemical shift translates into image blurring in all directions and signal loss. Due to the 2D readout gradients in these trajectories, aliasing artifacts happen from all directions resulting in additional streaks and swirls, therefore the FOV has to be chosen with attention to aliasing in all directions. Commonly mild undersampling artifacts are tolerated in order to reduce imaging time.

The readout of an EPI echo train also introduces a specific artifact related to the alternating sampling gradients. This artifact is commonly known as *Nyquist ghost* or *N/2 artifact* and it is created by a mixture of gradient imperfections, eddy currents, concomitant fields, receiver filter asymmetry or susceptibility. All these factors will cause mismatches between odd and even echoes resulting in some signal being displaced, in single-shot EPI by half the field of view across the image along the phase-encode direction. Measuring the mismatches and post-processing the acquired data usually correct this artifact. When using h-EPI techniques with multiple excitations per acquisition, then the phase discrepancy between odd and even lines may lead to multiple ghosts at smaller fractions of the phase-encode FOV.

1.5 T vs 3 T

Cardiac imaging at 3 T is becoming increasingly popular due to the potentially higher SNR and CNR (Contrast to Noise Ratio). At higher fields, some of the above mentioned

artifacts become even more problematic such as those caused by B_0 and B_1 field inhomogeneities or chemical shift. The potential increase in SNR, however, can be traded for example for higher parallel imaging accelerations resulting in quicker imaging acquisitions, which can potentially reduce motion artifacts; or enable higher spatial-resolutions which can for example make Gibbs artifacts less prominent.

Together with an increase of approximately twofold in SNR, there is also a quadruple increase in RF power absorption. Some sequences, such as bSSFP, may have to be used with a reduced flip-angle and higher TR than at 1.5 T, which increases B_0 inhomogeneity sensitivity and reduces contrast. Although T_2 relaxation times of tissues remain approximately unchanged from those at 1.5 T, T_1 relaxation times are noticeably longer at 3 T. This requires many protocols to be adapted for use at 3 T. For example the optimal inversion times for black blood imaging and late-Gd-enhancement may need to be increased. The same changes in relaxation time can also be used to reduce the dose of Gd contrast agent in first-pass perfusion and LGE studies decreasing possible susceptibility problems.

Cardiac gating can also be more challenging at 3 T. The higher field strength creates more magnetohydrodynamic distortion of the ECG signal, which can prevent the scanner from gating properly leading to additional artifacts.

Summary

Cardiovascular imaging is complicated primarily by the complex nature of the cardiac motion. Many of the cardiac imaging artifacts are directly related to motion or indirectly introduced by the requirement to shorten the acquisition time to remove motion. The complex cardiac structure with mixtures of fat and water based tissues containing complex and varying blood flows, and the large chest region with many organs and tissue-air interfaces also open the door to additional artifacts and measurement errors.

If we understand the physical principles behind the formation of artifacts, we should be in a position to identify and possibly avoid them, increasing image quality and reliability of interpretation.

References

1. Al-Kwifi O, Stainsby J, Foltz WD, Sussman MS, Huang Y, Wright G. Characterizing coronary motion and its effect on MR coronary angiography-initial experience. J Magn Reson Imaging. 2006;24(4):842–50.
2. Storey P, Chen Q, Li W, Edelman RR, Prasad PV. Band artifacts due to bulk motion. Magn Reson Med. 2002;48(6):1028–36.
3. Togawa T, Okai O, Oshima M. Observation of blood flow E.M.F. in externally applied strong magnetic field by surface electrodes. Med Biol Eng. 1967;5(2):169–70.
4. Setser RM, Fischer SE, Lorenz CH. Quantification of left ventricular function with magnetic resonance images acquired in real time. J Magn Reson Imaging. 2000;12(3):430–8.
5. Ferreira P, Gatehouse P, Kellman P, Bucciarelli-Ducci C, Firmin D. Variability of myocardial perfusion dark rim Gibbs artifacts due to sub-pixel shifts. J Cardiovasc Magn Reson. 2009; 11:17.
6. Di Bella EVR, Parker DL, Sinusas AJ. On the dark rim artifact in dynamic contrast-enhanced MRI myocardial perfusion studies. Magn Reson Med. 2005;54(5):1295–9.
7. Tsao J, Boesiger P, Pruessmann KP. k-t BLAST and k-t SENSE: dynamic MRI with high frame rate exploiting spatiotemporal correlations. Magn Reson Med. 2003;50(5):1031–42.
8. Plein S, Ryf S, Schwitter J, Radjenovic A, Boesiger P, Kozerke S. Dynamic contrast-enhanced myocardial perfusion MRI accelerated with k-t sense. Magn Reson Med. 2007;58(4): 777–85.
9. Otazo R, Kim D, Axel L, Sodickson DK. Combination of compressed sensing and parallel imaging for highly accelerated first-pass cardiac perfusion MRI. Magn Reson Med. 2010;64(3): 767–76.
10. Scheffler K, Lehnhardt S. Principles and applications of balanced SSFP techniques. Eur Radiol. 2003;13(11):2409–18.
11. Reeder SB, Faranesh AZ, Boxerman JL, McVeigh ER. In vivo measurement of T*2 and field inhomogeneity maps in the human heart at 1.5 T. Magn Reson Med. 1998;39(6):988–98.
12. Atalay MK, Poncelet BP, Kantor HL, Brady TJ, Weisskoff RM. Cardiac susceptibility artifacts arising from the heart-lung interface. Magn Reson Med. 2001;45(2):341–5.
13. Sorrell VL, Anderson JL, Gatehouse PD, Mohiaddin RH. Off-frequency tuning error artifact in steady-state free precession cine imaging due to adjacent air-filled bowel. J Cardiovasc Magn Reson. 2004;6(3):709–16.
14. Markl M, Alley MT, Elkins CJ, Pelc NJ. Flow effects in balanced steady state free precession imaging. Magn Reson Med. 2003;50(5):892–903.
15. Storey P, Li W, Chen Q, Edelman RR. Flow artifacts in steady-state free precession cine imaging. Magn Reson Med. 2004;51(1): 115–22.
16. Ferreira P, Gatehouse P, Bucciarelli-Ducci C, Wage R, Firmin D. Measurement of myocardial frequency offsets during first pass of a gadolinium-based contrast agent in perfusion studies. Magn Reson Med. 2008;60(4):860–70.
17. Ferreira PF, Gatehouse PD, Firmin DN. Myocardial first-pass perfusion imaging with hybrid-EPI: frequency-offsets and potential artefacts. J Cardiovasc Magn Reson. 2012;14:44.
18. Liao JR, Pauly JM, Brosnan TJ, Pelc NJ. Reduction of motion artifacts in cine MRI using variable-density spiral trajectories. Magn Reson Med. 1997;37(4):569–75.
19. Gatehouse PD, Firmin DN, Collins S, Longmore DB. Real time blood flow imaging by spiral scan phase velocity mapping. Magn Reson Med. 1994;31(5):504–12.
20. Rasche V, Holz D, Schepper W. Radial turbo spin echo imaging. Magn Reson Med. 1994;32(5):629–38.
21. Glover GH, Pauly JM. Projection reconstruction techniques for reduction of motion effects in MRI. Magn Reson Med. 1992;28(2):275–89.